*Inorg. Chem.* **1992,** *31,* 3718–3723

# Periodic Trends in Charge Distribution for Transition Metal Complexes Containing Catecholate and Semiquinone Ligands. Metal-Mediated Spin Coupling in the Bis(3,5-di-*tert*-butyl-1,2-semiquinone) Complexes of Palladium(II) and Platinum(II), $M(DBSQ)_2$ ($M = Pd, Pt$)

**Glenn A. Fox and Cortlandt G. Pierpont***

Department of Chemistry and Biochemistry, University of Colorado, Boulder, Colorado 80309

*Received February 5, 1992*

Reactions carried out with $M_2(DBA)_3$ (M = Pd, Pt; DBA = dibenzylideneacetone) and 3,5-di-*tert*-butyl-1,2-benzoquinone gave as major products the $M(DBSQ)_2$ complexes. Crystallographic characterization on both complexes showed that they are monomeric, with square planar geometries for the metals and metrical values that reflect the semiquinone character of the ligands and the divalent charges of the metal ions. Both complexes appear diamagnetic in magnetic susceptibility measurements. However, paramagnetic broadening and shifting of *tert*-butyl $^1H$-NMR resonances of $Pd(DBSQ)_2$ shows the effect of residual, low-level paramagnetism. Resonances of $Pt(DBSQ)_2$ are sharp indicating stronger radical–radical exchange through the Pt ion and complete diamagnetism for the complex. Electrochemical characterization shows that both complexes undergo two reversible reductions and one irreversible oxidation. A minor product obtained from the synthesis of $Pd(DBSQ)_2$ was characterized structurally and found to be $Pd_2[Pd(DBSQ)_2]_2$. The complex molecule consists of two planar *cis*-$Pd(DBSQ)_2$ units bridged by two Pd atoms $\pi$-bonded to allylic regions of the DBSQ ligands. A minor product was also obtained from the synthesis of $Pt(DBSQ)_2$. This complex is paramagnetic and EPR active, giving a spectrum with hyperfine coupling that may be described as a single DBSQ ligand coupled to a diamagnetic Pt atom. Otherwise, the form of this product remains unclear. The localized charge distribution of $Pd(DBSQ)_2$ and $Pt(DBSQ)_2$ is quite different from the delocalized electronic structures of the diimine and 1,2-dithiolene analogs studied earlier. Differences in magnetic coupling illustrate the metal dependence of the SQ–SQ exchange interaction through the two metals. The complexes illustrate the shift in charge distribution for transition metal quinone complexes across the second and third transition series of the periodic table.

## Introduction

The coordination chemistry of semiquinone and catecholate complexes containing transition metal ions has developed enormously over the past 15 years. Many of the most interesting and important properties of these compounds are related to the balance of energy between metal and quinone electronic levels. Charge delocalization contributes in a much less important way to the electronic structures of the quinone complexes than to the corresponding members of the 1,2-dithiolene and diimine series that were the subjects of intense study during the 1960s.[1] The combination of a localized electronic structure with similarity in localized orbital energies gives rise to a number of unique properties, including low-energy charge-transfer transitions that sometimes extend well into the near-IR,[2] selective electrochemical activity at either the ligand or metal,[3] magnetic exchange between semiquinone radical ligands and the coordinated metal ion,[4] and general questions concerning charge distribution within the complex molecule.[5] Charge distribution has been found to follow a periodic pattern in the neutral homoleptic complexes of the catecholate and semiquinone ligands.[5] Metal ions of the first transition series form complexes containing partially reduced semiquinone ligands, while the larger metals of the second and third rows with higher d-orbital energies form catecholate complexes with metal ions in high oxidation states. This trend is illustrated by the Cr, Mo, W[6] and Mn, Tc, Re[7] congenic groups where the Cr and Mn complexes form $Mn^{II}(SQ)_2$ and $Cr^{III}(SQ)_3$ species, while the related complexes formed with the larger metals are $M^{VI}(Cat)_3$. Periodic changes in metal orbital energy across a transition series also result in changes in charge distribution,[5] and the present project was carried out partially in the interest of illustrating this property.

Other interests in developing the quinone complexes of Pd and Pt are related to potentially interesting and important properties as solid-state materials[8] and as chemotherapeutic agents.[9] Intrastack oxidation that contributes to the one-dimensional conductive properties of cyano and oxalato complexes of Pt may be affected without an external oxidant through Pt–semiquinone electron transfer within the molecules that form the stack of interacting, planar $Pt(SQ)_2$ units.[2] The affinity of planar quinone ligands for planar, unsaturated base molecules for charge-transfer complexation makes the Pd and Pt complexes excellent candidates for biological intercalation studies.[10] A more direct interest in these compounds concerns their relationship with related 1,2-dithiolene and diimine complexes (I). The neutral bis(*o*-phenylenediimine)nickel complex, first reported by Feigl and Furth,[11] and its Pd and Pt analogs are paradigms for metal–

---

(1) (a) McCleverty, J. A. *Prog. Inorg. Chem.* **1968**, *10*, 49. (b) Schrauzer, G. N. *Acc. Chem. Res.* **1969**, *2*, 72.

(2) (a) Haga, M.; Dodsworth, E. S.; Lever, A. B. P.; Boone, S. R.; Pierpont, C. G. *J. Am. Chem. Soc.* **1986**, *108*, 7413. (b) Lange, C. W.; Foldeaki, M.; Nevodchikov, V. I.; Cherkasov, V. K.; Abakumov, G. A.; Pierpont, C. G. *J. Am. Chem. Soc.* **1992**, *114*, 4220.

(3) Bhattacharya, S.; Pierpont, C. G. *Inorg. Chem.* **1992**, *31*, 35.

(4) Lynch, M. W.; Buchanan, R. M.; Pierpont, C. G.; Hendrickson, D. N. *Inorg. Chem.* **1981**, *20*, 1038.

(5) Bhattacharya, S.; Boone, S. R.; Fox, G. A.; Pierpont, C. G. *J. Am. Chem. Soc.* **1990**, *112*, 1088.

(6) (a) Buchanan, R. M.; Kessel, S. L.; Downs, H. H.; Pierpont, C. G.; Hendrickson, D. N. *J. Am. Chem. Soc.* **1978**, *100*, 7894. (b) deLearie, L. A.; Pierpont, C. G. *Inorg. Chem.* **1988**, *27*, 3842.

(7) (a) Lynch, M. W.; Hendrickson, D. N.; Fitzgerald, B. J.; Pierpont, C. G. *J. Am. Chem. Soc.* **1984**, *106*, 2041. (b) deLearie, L. A.; Haltiwanger, R. C.; Pierpont, C. G. *J. Am. Chem. Soc.* **1989**, *111*, 4324. (c) deLearie, L. A.; Haltiwanger, R. C.; Pierpont, C. G. *Inorg. Chem.* **1987**, *26*, 817.

(8) Clemenson, P. I. *Coord. Chem. Rev.* **1990**, *106*, 171.

(9) Schwartz, P.; Troy, A. L.; Gale, G. R. Presented at the 192nd National Meeting of the American Chemical Society, Anaheim, CA, Sept 7–12, 1986; Abstract INOR 133.

(10) (a) Pyle, A. M.; Barton, J. K. *Prog. Inorg. Chem.* **1990**, *38*, 413. (b) Foster, R.; Foreman, M. I. *Chemistry of Quinoid Compounds, Part I*; John Wiley: New York, 1974; p 257.

(11) Feigl, F.; Furth, M. *Monatsh. Chem.* **1927**, *48*, 445.

0020-1669/92/1331-3718$03.00/0

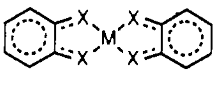

X = O, NH, S
M = Ni, Pd, Pt

I

ligand delocalization.[12] Detailed characterization on the neutral bis(1,2-dithiolene) complexes of Ni, Pd, and Pt revealed that these complexes shared the delocalized electronic structures of the diimine complexes.[1] As the oxygen analogs of this series, it was of interest to determine whether the properties of the neutral quinone complexes of Pd and Pt were similar to the diimine and dithiolene analogs in electronic structure or whether their properties would indicate a more localized charge distribution.

## Experimental Section

**Materials.** 3,5-Di-*tert*-butyl-1,2-benzoquinone (DBBQ)[13] and dibenzylideneacetone (DBA) were purchased from Aldrich. $Pd_2(DBA)_3$ and $Pt_2(DBA)_3$ were prepared by literature procedures.[14]

**Complex Syntheses. Pd(DBSQ)$_2$ and Pd$_2$[Pd(DBSQ)$_2$]$_2$.** A degassed solution containing 0.11 g (0.54 mmol) of DBBQ in $CH_2Cl_2$ (20 mL) was added to a degassed solution consisting of 0.14 g (0.13 mmol) of $Pd_2(DBA)_3$ dissolved in $CH_2Cl_2$ (30 mL). The mixture was warmed and stirred under $N_2$ for 4 h as the color changed to dark blue. The mixture was then chromatographed using a silica gel column with dichloromethane as the eluent. Fractions obtained included yellow DBA, a large blue fraction containing Pd(DBSQ)$_2$, and a small blue fraction containing Pd$_2$[Pd(DBSQ)$_2$]$_2$. It was noted that Pd(DBSQ)$_2$ showed a tendency to decompose on the column. Consequently, the separation procedure should be carried out as rapidly as possible. Both Pd(DBSQ)$_2$ and Pd$_2$[Pd(DBSQ)$_2$]$_2$ were recrystallized from dichloromethane giving yields of Pd(DBSQ)$_2$ that were typically 55–70% and yields of Pd$_2$[Pd(DBSQ)$_2$]$_2$·$CH_2Cl_2$ that were less than 5%.

**Pt(DBSQ)$_2$.** A degassed solution containing 0.12 g (0.55 mmol) of DBBQ in $CH_2Cl_2$ (20 mL) was added to a degassed solution consisting of 0.15 g (0.14 mmol) of $Pt_2(DBA)_3$ dissolved in $CH_2Cl_2$ (30 mL). The mixture was warmed and stirred under $N_2$ for 4 h as the color changed to dark blue. The mixture was then chromatographed using a silica gel column with dichloromethane as the eluent. Fractions obtained included yellow DBA, a blue fraction containing *trans*-Pt(DBSQ)$_2$, and a blue fraction containing *cis*-Pt(DBSQ)$_2$. A wine-red product remained on the column. This product was isolated using methanol as the eluent. The yield of Pt(DBSQ)$_2$ obtained was typically 60% using this procedure; the red product is obtained in low yield (<5%).

**Physical Measurements.** Electronic spectra were recorded on a Perkin-Elmer Lambda 9 spectrophotometer. Infrared spectra were obtained on an IBM IR/30 FTIR spectrometer with samples prepared as KBr pellets. $^1H$-NMR spectra were recorded on a Varian VXR 300S spectrometer. EPR spectra were recorded on a Varian E-109 spectrometer and reference to DPPH as the *g*-value standard. Cyclic voltammograms were obtained with a Cypress CYSY-1 computer-controlled electroanalysis system. A platinum disk working electrode and a platinum wire counter electrode were used. A Ag/Ag$^+$ reference electrode was used that consisted of a $CH_2Cl_2$ solution of $AgPF_6$ in contact with a silver wire placed in glass tubing with a Vycor frit at one end to allow ion transport. Tetrabutylammonium hexafluorophosphate (TBHP) was used as the supporting electrolyte, and the ferrocene/ferrocenium couple was used as an internal standard. With this experimental arrangement the Fc/Fc$^+$ couple appeared at 0.170 V (vs Ag/Ag$^+$) with $\Delta E$ of 65 mV.

**Crystallographic Structure Determination on Pd(DBSQ)$_2$.** Dark blue crystals of Pd(DBSQ)$_2$ were obtained as rhombic blocks from a 1:2 dichloromethane/hexane solution. Axial photographs indicated monoclinic symmetry, and the centered settings of 25 reflections with $2\theta$ values in the range between 25 and 35° gave the unit cell dimensions listed in Table I. Data were collected by $\theta$–$2\theta$ scans within the angular range 3.0–45.0°. The Pd atom is required to lie at the origin of the unit cell. Phases generated from a structure factor calculation including only the Pd atom gave the locations of the carbon and oxygen atoms of the semiquinone ligand. Final cycles of least-squares refinement converged with discrepancy indices of $R = 0.029$ and $R_w = 0.041$. Final positional parameters for atoms of the complex molecule are listed in Table II. Tables containing a full listing of atom positions, anisotropic displacement parameters, and hydrogen atom locations are available as supplementary material.

**Crystallographic Structure Determination on Pd$_2$[Pd(DBSQ)$_2$]$_2$·CH$_2$Cl$_2$.** Dark blue crystals of Pd$_2$[Pd[Pd(DBSQ)$_2$]$_2$ were obtained as thin plates from a dichloromethane solution. Axial photographs indicated monoclinic symmetry, and the centered settings of 25 reflections with $2\theta$ values in the range between 21 and 25° gave the unit cell dimensions listed in Table I. Data were collected by $\theta$–$2\theta$ scans within the angular range 3.0–45.0°. The locations of the four independent Pd atoms and the oxygen and ring carbon atoms of the semiquinone ligands were determined using direct methods. The crystal structure consists of two independent Pd$_2$[Pd(DBSQ)$_2$]$_2$ complex molecules, each located about crystallographic inversion centers, and a $CH_2Cl_2$ solvate molecule. Final cycles of least-squares refinement converged with discrepancy indices of $R = 0.071$ and $R_w = 0.085$. Final positional parameters for atoms of the complex molecule are listed in Table III. Tables containing a full listing of atom positions, anisotropic displacement parameters, and hydrogen atom locations are available as supplementary material.[15]

**Crystallographic Structure Determination on Pt(DBSQ)$_2$.** Dark blue crystals of Pt(DBSQ)$_2$ were obtained as rhombic blocks from a 1:2 dichloromethane/hexane solution. Axial photographs indicated monoclinic symmetry, and the centered settings of 25 reflections with $2\theta$ values in the range between 25 and 35° gave the unit cell dimensions listed in Table I. Data were collected by $\theta$–$2\theta$ scans within the angular range 3.0–45.0°. The complex was determined to be isostructural with the Pd analog. Atom locations used for this structure determination were used in initial cycles of refinement on Pt(DBSQ)$_2$. Final cycles of least-squares refinement converged with discrepancy indices of $R = 0.025$ and $R_w = 0.031$. Final positional parameters for atoms of the complex molecule are listed in Table IV. Tables containing a full listing of atom positions, anisotropic displacement parameters, and hydrogen atom locations are available as supplementary material.

## Experimental Results

Several synthetic routes to the quinone complexes of Pd and Pt were considered. Two procedures beginning with complexes of the divalent metal ions were attempted unsuccessfully. Addition of a basic solution of 3,5-di-*tert*-butylcatechol to a solution containing $MCl_4^{2-}$ (M = Pd, Pt) gave only the benzoquinone and the metallic form of the metal ion. Additionally, treatment of $Pd(C_6H_5CN)_2Cl_2$ and Pt(COD)Cl$_2$ with thallium and lithium salts of the semiquinone gave similar results. A route that had proved successful for a number of other metals, including nickel, involved treating the metal carbonyl with the benzoquinone form of the ligand. Simple carbonyl complexes of Pd and Pt are not readily available, but the olefin complexes of the zerovalent metals formed with dibenzylideneacetone are easily prepared[14] and were found to react with 3,5-di-*tert*-butyl-1,2-benzoquinone (DBBQ) under mild conditions. The products of these reactions are described below.

**Pd(3,5-DBSQ)$_2$.** Chromatographic separation of the material obtained by heating $Pd_2(DBA)_3$ with 3,5-DBBQ in toluene gave two dark blue complexes in crystalline form. Structural characterization on crystals obtained from the first blue fraction formed in greatest yield from the synthetic procedure revealed that the product was Pd(DBSQ)$_2$. A view of the complex molecule is shown in Figure 1; bond distances and angles are listed in Table V. The molecule is square planar and monomeric. Quinone *tert*-butyl substituents are in a trans disposition in the isomer characterized crystallographically. Oxygen bond lengths to the metal are 1.977 (3) and 1.982 (3) Å, typical values for Pd(II).[16] Accordingly, the C–O bond lengths of the ligands are 1.302 (5)

---

[12] Balch, A. L.; Holm, R. H. *J. Am. Chem. Soc.* **1966**, *88*, 5201.

[13] Abbreviations: BQ, SQ, and Cat have been used to refer to benzoquinone, semiquinone, and catecholate forms of the quinone ligands; DB- has been used as a prefix for the substituted 3,5-di-*tert*-butyl quinone ligands.

[14] (a) Ukai, T.; Kawazura, H.; Ishii, Y.; Bonnet, J. J.; Ibers, J. A. *J. Organomet. Chem.* **1974**, *65*, 253. (b) Cherwinski, W. J.; Johnson, B. F. G.; Lewis, J. *J. Chem. Soc., Dalton Trans.* **1974**, 1405.

[15] The results of the structure determination on Pd$_2$[Pd(DBSQ)$_2$]$_2$ were communicated previously: Fox, G. A.; Pierpont, C. G. *J. Chem. Soc., Chem. Commun.* **1988**, 806.

**Table I.** Crystallographic Data for Pd(DBSQ)$_2$, Pd$_2$[Pd(DBSQ)$_2$]$_2$, and Pt(DBSQ)$_2$[a]

| | Pd(DBSQ)$_2$ | Pd$_2$[Pd(DBSQ)$_2$]$_2$·CH$_2$Cl$_2$ | Pt(DBSQ)$_2$ |
|---|---|---|---|
| mol wt | 547.0 | 1388.9 | 635.7 |
| color | blue | blue | blue |
| cryst system | monoclinic | monoclinic | monoclinic |
| space group | $P2_1/c$ | $P2_1/c$ | $P2_1/c$ |
| $a$ (Å) | 9.316 (2) | 15.534 (6) | 9.403 (1) |
| $b$ (Å) | 12.716 (3) | 19.978 (8) | 12.684 (2) |
| $c$ (Å) | 12.062 (3) | 19.604 (7) | 12.016 (2) |
| $\beta$ (deg) | 99.68 (2) | 91.52 (3) | 100.11 (2) |
| $V$ (Å$^3$) | 1408.5 (9) | 6081 (2) | 1410.8 (6) |
| $Z$ | 2 | 4 | 2 |
| $D_{\text{calcd}}$ (g cm$^{-3}$) | 1.290 | 1.426 | 1.496 |
| $D_{\text{exptl}}$ (g cm$^{-3}$) | 1.31 | 1.46 | 1.52 |
| $\mu$ (mm$^{-1}$) | 0.676 | 1.270 | 5.050 |
| $T_{\min}$, $T_{\max}$ | 0.821, 0.965 | 0.638, 0.985 | 0.822, 0.956 |
| $R$, $R_w$[b] | 0.029, 0.041 | 0.071, 0.084 | 0.025, 0.031 |
| GOF | 1.18 | 1.36 | 0.81 |

[a] Radiation, Mo K$\alpha$ (0.710 73 Å); temperature, 294–297 K. [b] $R = \sum||F_o| - |F_c||/\sum|F_o|$. $R_w = [\sum w(|F_o| - |F_c|)^2/\sum w(F_o)^2]^{1/2}$.

**Table II.** Atomic Coordinates (×10$^4$) and $U_{eq}$ values (Å$^2$) for Selected Atoms of Pd(DBSQ)$_2$

| atom | $x/a$ | $y/b$ | $z/c$ | $U_{eq}$ |
|---|---|---|---|---|
| Pd | 0 | 0 | 0 | 45 (1) |
| O1 | 2016 (3) | 156 (2) | 824 (2) | 51 (1) |
| O2 | 744 (3) | –1376 (2) | –413 (2) | 48 (1) |
| C1 | 2803 (4) | –669 (3) | 702 (3) | 45 (1) |
| C2 | 2109 (4) | –1516 (3) | 31 (3) | 41 (1) |
| C3 | 2888 (4) | –2457 (3) | –97 (3) | 42 (1) |
| C4 | 4294 (4) | –2491 (3) | 459 (3) | 46 (1) |
| C5 | 5018 (4) | –1654 (3) | 1131 (3) | 43 (1) |
| C6 | 4267 (4) | –745 (3) | 1228 (3) | 46 (1) |

**Table III.** Atomic Coordinates (×10) and $U_{eq}$ Values (Å$^2$) for Selected Atoms of Pd$_2$[Pd(DBSQ)$_2$]$_2$

| atom | $x/a$ | $y/b$ | $z/c$ | $U_{eq}$ |
|---|---|---|---|---|
| Pd1 | 4423 (2) | 5025 (1) | 9224 (1) | 48 (1) |
| Pd2 | 7033 (2) | 4089 (2) | 9110 (1) | 65 (1) |
| O1 | 3888 (13) | 5912 (10) | 9231 (9) | 55 (6) |
| O2 | 3390 (12) | 4786 (10) | 9767 (10) | 58 (7) |
| O3 | 5436 (12) | 5280 (11) | 8656 (10) | 58 (7) |
| O4 | 4920 (12) | 4129 (10) | 9167 (10) | 58 (6) |
| C1 | 3158 (19) | 5938 (15) | 9559 (15) | 47 (9) |
| C2 | 2891 (18) | 5332 (15) | 9852 (14) | 42 (9) |
| C3 | 2085 (16) | 5262 (13) | 10243 (13) | 28 (8) |
| C4 | 1710 (18) | 5876 (14) | 10283 (14) | 47 (9) |
| C5 | 1917 (19) | 6487 (15) | 9951 (15) | 49 (10) |
| C6 | 2653 (18) | 6514 (16) | 9563 (14) | 44 (9) |
| C15 | 5807 (18) | 4732 (16) | 8487 (14) | 44 (9) |
| C16 | 5596 (19) | 4133 (16) | 8756 (15) | 52 (10) |
| C17 | 5939 (18) | 3490 (15) | 8556 (14) | 47 (9) |
| C18 | 6651 (21) | 3594 (16) | 8112 (15) | 66 (11) |
| C19 | 6876 (18) | 4188 (16) | 7786 (14) | 53 (10) |
| C20 | 6447 (16) | 4765 (14) | 7949 (13) | 39 (9) |
| Pd3 | 507 (2) | 5738 (2) | 5001 (1) | 56 (1) |
| Pd4 | 1825 (2) | 4359 (2) | 6387 (2) | 77 (1) |
| O5 | –704 (12) | 6062 (10) | 5042 (9) | 55 (6) |
| O6 | 374 (11) | 5906 (9) | 4019 (9) | 42 (6) |
| O7 | 1747 (11) | 5485 (10) | 5008 (9) | 46 (6) |
| O8 | 699 (13) | 5664 (10) | 6027 (9) | 57 (6) |
| C29 | 349 (16) | 6155 (13) | 3845 (13) | 30 (8) |
| C30 | –962 (20) | 6299 (15) | 4405 (15) | 50 (10) |
| C31 | –1786 (22) | 6577 (18) | 4297 (17) | 71 (12) |
| C32 | –1988 (21) | 6734 (15) | 3582 (15) | 58 (10) |
| C33 | –1284 (18) | 6725 (15) | 3106 (14) | 48 (10) |
| C34 | –541 (19) | 6484 (15) | 3249 (14) | 50 (10) |
| C43 | 2133 (19) | 5405 (16) | 5570 (15) | 57 (10) |
| C44 | 1505 (21) | 5462 (16) | 6175 (15) | 53 (10) |
| C45 | 1806 (19) | 5393 (15) | 6872 (14) | 41 (9) |
| C46 | 2650 (19) | 5157 (15) | 6903 (15) | 56 (10) |
| C47 | 3278 (21) | 5119 (17) | 6383 (17) | 71 (11) |
| C48 | 3019 (18) | 5284 (15) | 5742 (15) | 49 (10) |

**Table IV.** Atomic Coordinates (×10$^4$) and $U_{eq}$ Values (Å$^2$) for Selected Atoms of Pt(DBSQ)$_2$

| atom | $x/a$ | $y/b$ | $z/c$ | $U_{eq}$ |
|---|---|---|---|---|
| Pt | 0 | 0 | 0 | 41 (1) |
| O1 | 1998 (6) | 140 (3) | 821 (4) | 49 (2) |
| O2 | 759 (6) | –1362 (5) | –407 (5) | 47 (2) |
| C1 | 2814 (9) | –678 (6) | 690 (7) | 40 (2) |
| C2 | 2117 (7) | –1523 (6) | 27 (6) | 38 (2) |
| C3 | 2882 (8) | –2457 (7) | –95 (7) | 41 (2) |
| C4 | 4297 (8) | –2493 (7) | 460 (7) | 47 (2) |
| C5 | 5000 (8) | –1658 (7) | 1134 (6) | 43 (2) |
| C6 | 4269 (8) | –752 (7) | 1233 (7) | 46 (2) |

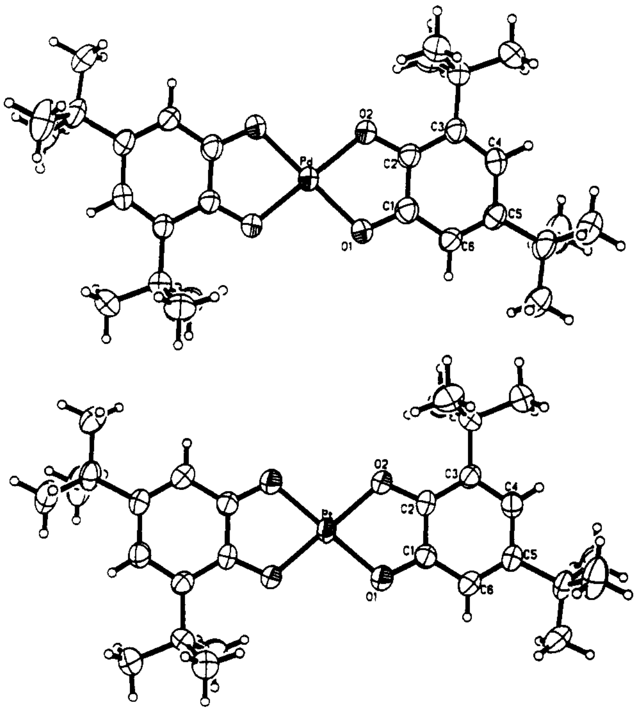

**Figure 1.** Views of the Pd(DBSQ)$_2$ and Pt(DBSQ)$_2$ complex molecules.

and 1.307 (4) Å, values that are commonly found for semiquinone ligands.[17] Further, the pattern of C–C bond lengths within the quinone ring, with the shortest values at bonds that would be double bonds for the benzoquinone, agrees with the semiquinone charge of the ligands. The deep blue color of the complex results from an intense charge-transfer band at 840 nm (13 000 M$^{-1}$ cm$^{-1}$) (Table VI). Cyclic voltammetry on Pd(DBSQ)$_2$ shows that the complex undergoes two reversible reductions at –0.244

---

(16) Siedle, A. R.; Newmark, P. A.; Pignolet, L. H. *J. Am. Chem. Soc.* **1982**, *104*, 6584.

(17) Boone, S. R.; Purser, G. H.; Chang, H.-R.; Lowery, M. D.; Hendrickson, D. N. *J. Am. Chem. Soc.* **1989**, *111*, 2292.

**Table V.** Selected Bond Lengths and Angles for $Pd(DBSQ)_2$ and $Pt(DBSQ)_2$

| $Pd(DBSQ)_2$ | | $Pt(DBSQ)_2$ | |
|---|---|---|---|
| | Lengths (Å) | | |
| Pd–O1 | 1.982 (3) | Pt–O1 | 1.963 (6) |
| Pd–O2 | 1.977 (3) | Pt–O2 | 1.971 (6) |
| C1–O1 | 1.302 (5) | C1–O1 | 1.317 (8) |
| C2–O2 | 1.307 (4) | C2–O2 | 1.308 (8) |
| C1–C2 | 1.435 (5) | C1–C2 | 1.425 (11) |
| C2–C3 | 1.420 (5) | C2–C3 | 1.406 (11) |
| C3–C4 | 1.368 (5) | C3–C4 | 1.381 (10) |
| C4–C5 | 1.436 (5) | C4–C5 | 1.424 (11) |
| C5–C6 | 1.366 (5) | C5–C6 | 1.355 (12) |
| C6–C1 | 1.407 (5) | C6–C1 | 1.412 (11) |
| | Angles (deg) | | |
| O1–Pd–O2 | 82.7 (1) | O1–Pt–O2 | 81.3 (12) |
| O1–Pd–O2′ | 97.3 (1) | O1–Pt–O2′ | 98.7 (12) |
| Pd–O1–C1 | 111.5 (2) | Pt–O1–C1 | 113.1 (10) |
| Pd–O2–C2 | 112.1 (2) | Pt–O2–C2 | 114.2 (5) |

**Table VI.** Spectral and Electrochemical Properties of $Pd(DBSQ)_2$ and $Pt(DBSQ)_2$

| compd | λ (nm) ($\epsilon$ ($M^{-1}$ $cm^{-1}$))[a] | $E_{1/2}$ (V) vs $Fc/Fc^+$ ($\Delta E_p$ (mV))[a] |
|---|---|---|
| $Pd(DBSQ)_2$ | 296 (23 000), 382 (2500), 840 (13 000) | oxidn, +0.563;[b] redn, –0.244 (64), –0.865 (79) |
| $Pt(DBSQ)_2$ | 290 (5300), 493 (1250), 649 (1500), 719 (2500), 913 (21 000) | oxidn, +0.691;[b] redn, –0.059 (72), –0.802 (85) |

[a] Dichloromethane solutions. [b] Irreversible oxidation.

and –0.865 V (vs $Fc/Fc^+$) and one irreversible oxidation at +0.563 V. All of these processes are ligand based,[3] with the two reductions corresponding to stepwise formation of $Pd(DBSQ)(DBCat)^-$ and $Pd(DBCat)_2^{2-}$. Chemical reduction of the neutral complex using $CoCp_2$ gave an EPR-active species after addition of 1 equiv of reductant. The *g*-value of the signal was near 2.00 and the half-signal width was 8 G, but it was not possible to resolve hyperfine coupling. It was also not possible to isolate the products of reduction in pure form for further characterization.

As a complex containing two paramagnetic radical ligands "bridged" by a diamagnetic ligand, the magnetic properties of $Pd(DBSQ)_2$ are of interest. Magnetic susceptibility measurements on solid samples of the complex indicated that the complex was diamagnetic. However, NMR spectra recorded on the complex in solution indicate low-level paramagnetism. This appears as marked broadening of the *tert*-butyl resonances and temperature-dependent chemical shift values. In $CD_2Cl_2$ at –80 °C two broad resonances appear at 1.25 and 1.40 ppm. Upon increase of the temperature of the solution, the lower frequency resonance moves slightly down field to 1.35 ppm at 25 °C while the higher frequency resonance moves more markedly down field to 2.78 ppm. In toluene-$d_8$ solution the temperature-dependent shift is even more pronounced. At 100 °C the *tert*-butyl resonances appear at 1.50 and 3.45 ppm. As temperature is decreased, the upfield resonance remains essentially fixed in position, while the downfield resonance moves across the upfield resonance to 1.03 ppm at –85 °C. Shifts over the temperature range from +50 to –80 °C are shown in Figure 2. The resonance of one ring proton may also be seen in these spectra; the other appears to have been broadened into the baseline. In $CD_2Cl_2$ it may be seen as a broad resonance at 7.8 ppm at 0 °C with an upfield shift to 6.75 ppm at –80 °C. In toluene-$d_8$ this resonance appears at 6.55 ppm at –85 °C. At room temperature in both solvents this resonance is also broadened into the baseline. EPR spectra recorded on the 3,5-di-*tert*-butyl-1,2-semiquinone radical commonly show proton hyperfine coupling with the ring proton at the 4-position and the protons of the *tert*-butyl group at the 5-position of the ring.[18] The concentration of spin density at the C4–C5 bond of the ring in both free and complexed forms of the semiquinone enables tentative assignment of the paramagnetic NMR resonances of $Pd(DBSQ)_2$. The *tert*-butyl resonance that shows the greatest shifts with temperature is located on the carbon atom at the 5-position of the ring. A plot of the measured chemical shift values vs $1/T$ over the temperature range from –85 to +150

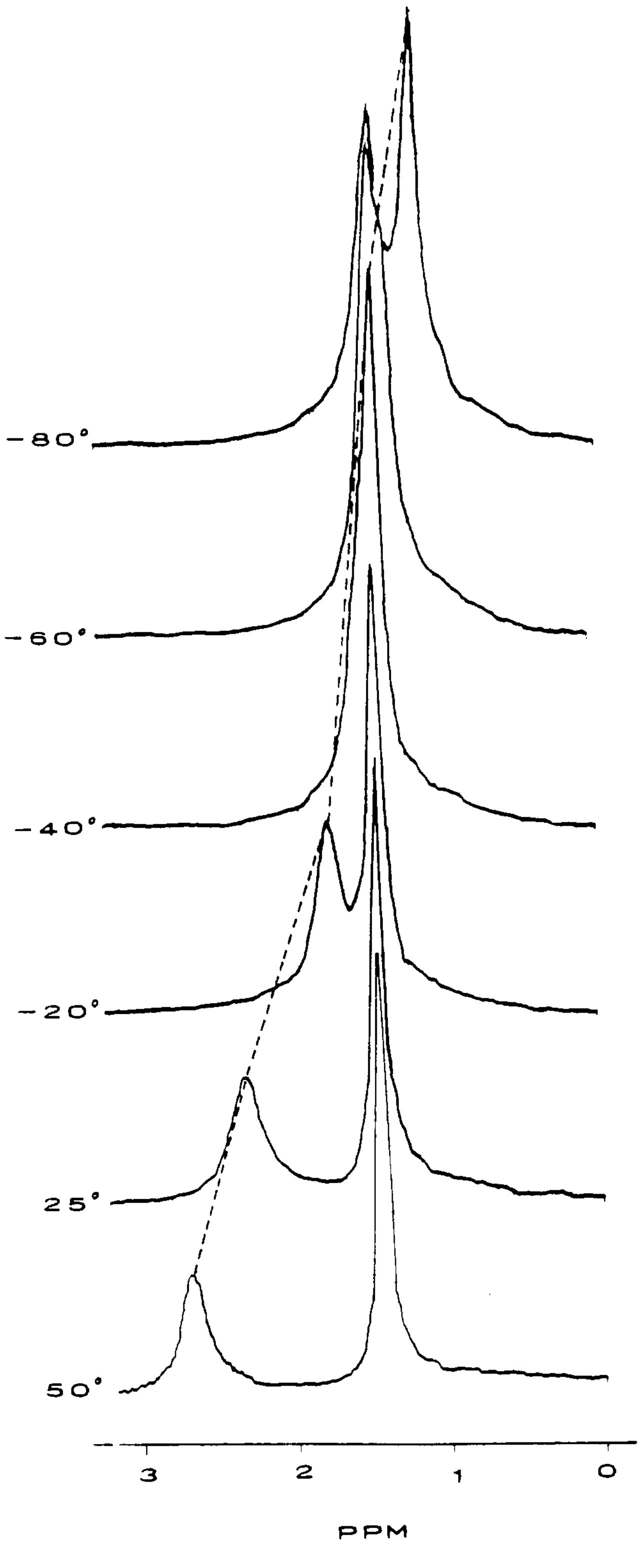

**Figure 2.** Temperature-dependent $^1$H-NMR spectra of $Pd(DBSQ)_2$ in the region of the *tert*-butyl resonances. Spectra were recorded in toluene-$d_8$.

---

(18) Pedersen, J. A. *Handbook of EPR Spectra from Quinones and Quinols*; CRC Press: Boca Raton, FL, 1985.

**Table VII.** Temperature-Dependent Chemical Shift Values for the Protons of the *tert*-Butyl Groups at the 5-Positions of the Semiquinone Rings of $Pd(DBSQ)_2$ Recorded in Toluene-$d_8$

| $T$ (°C) | $\delta$ (ppm) | $T$ (°C) | $\delta$ (ppm) |
|---|---|---|---|
| 150 | 3.75 | -30 | 1.65 |
| 100 | 3.45 | -40 | 1.48 |
| 75 | 3.08 | -50 | 1.41 |
| 50 | 2.71 | -60 | 1.35 |
| 25 | 2.31 | -70 | 1.22 |
| 0 | 2.05 | -80 | 1.15 |
| -20 | 1.75 | -85 | 1.13 |

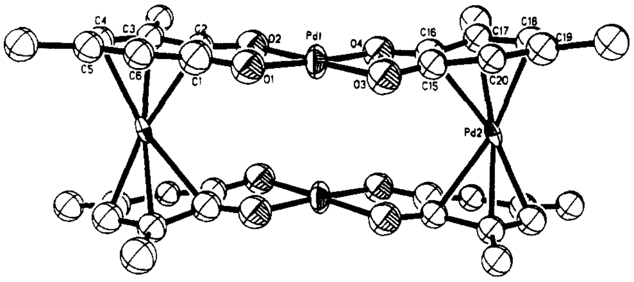

**Figure 3.** Structural features of $Pd_2[Pd(DBSQ)_2]_2$.

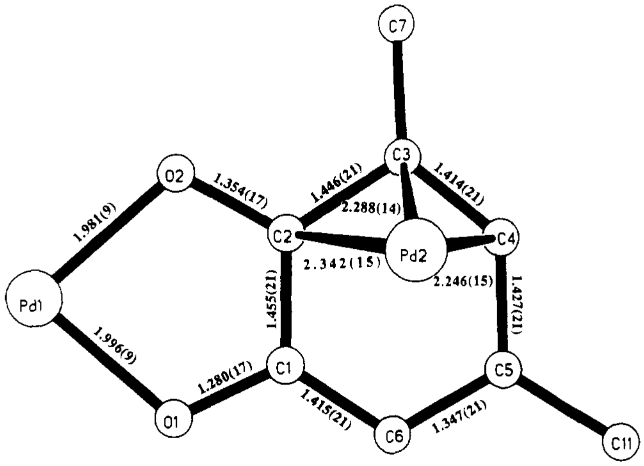

**Figure 4.** Average bond lengths (Å) with esd's for $Pd_2[Pd(DBSQ)_2]_2$.

°C listed in Table VII is reasonably linear. This may indicate simple Curie behavior, although the effect of antiferromagnetic exchange between radical ligands may also contribute to the temperature dependence of the shift.

**$Pd_2[Pd(DBSQ)_2]_2$.** Crystals of the second blue fraction obtained in low yield from chromatography on the products of the $Pd_2(DBA)_3$/DBBQ reaction form as thin plates. Our inability to obtain crystals with large volume has limited the quality of the structure determination on this product, but the results of crystallographic characterization clearly demonstrate the features of the molecule. A view of $Pd_2[Pd(DBSQ)_2]_2$ is shown in Figure 3. Average values for bond distances are illustrated in Figure 4. The $Pd_2[Pd(DBSQ)_2]_2$ molecule consists of two planar *cis*-Pd-$(DBSQ)_2$ units bridged by two Pd atoms. The Pd atoms are "sandwiched" between semiquinone rings of adjacent $Pd(DBSQ)_2$ units with three Pd–C lengths that are less than 2.5 Å and an allylic structure for the semiquinone rings (II). The pattern of

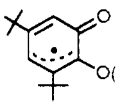

II

C–C and C–O lengths within the semiquinone ligands is in accord with this somewhat unconventional electronic structure of the semiquinones. In particular, there is a marked difference between average values for the C–O lengths, 1.280 (17) and 1.354 (17) Å, and the average C5–C6 length within the ring (1.347 (12) Å) is shorter than other C–C lengths. Palladium–carbon lengths to the three allylic carbon atoms of the ring average 2.246 (15), 2.288 (14), and 2.342 (15) Å. These values are 0.1 Å longer than Pd–C values reported for $Pd((CH_2)_2CMe)_2$[19] and allylic complexes of Pd(II), reflecting the zerovalent character of the bridging Pd atoms. Distances to the olefin carbon atoms of $Pd(DBA)_3$ average 2.23 (2) Å for Pd(0). The $^1$H-NMR spectrum of $Pd_2[(DBSQ)_2]_2$ shows two sharp *tert*-butyl resonances at 1.03 and 1.41 ppm and ring proton resonances at 5.63 and 5.69 ppm, in accord with the diamagnetism of the complex.

**$Pt(DBSQ)_2$.** Treatment of $Pt_2(DBA)_3$ with DBBQ in dichloromethane gave $Pt(DBSQ)_2$ in high yield. The complex is dark blue in color, similar to the Pd analog, and shows intense bands at 493 nm (1250 $M^{-1}$ $cm^{-1}$), 719 (2500), and 913 (21 000). Crystallographic characterization on the complex has shown that it is isostructural with $Pd(DBSQ)_2$. A view of the complex molecule is shown in Figure 1; bond distances and angles are listed in Table V. The two Pt–O lengths are slightly shorter than Pd–O lengths in $Pd(DBSQ)_2$; otherwise, the Pt and Pd complexes are nearly identical. NMR spectra of $Pt(DBSQ)_2$ are clearly resolved and fail to show the broadening seen for spectra of Pd-$(DBSQ)_2$. Furthermore, cis and trans isomers of the complex could be separated chromatographically. The trans isomer, characterized crystallographically, shows sharp *tert*-butyl resonances at 1.455 and 1.259 ppm and two resonances at 7.05 and 6.84 ppm coupled by 2 Hz. The cis isomer shows sharp *tert*-butyl resonances at 1.465 and 1.261 ppm and ring proton resonances at 6.96 and 6.83 ppm, coupled by 2 Hz. Electrochemical characterization on $Pt(DBSQ)_2$ produced results that were similar to those for $Pd(DBSQ)_2$ but with potentials shifted positively. The complex undergoes reversible reduction in two steps at −0.059 and −0.802 V and shows an irreversible oxidation at +0.691 V. Chemical reduction of $Pt(DBSQ)_2$ using $CoCp_2$ failed to yield characterizable reduction products of the complex.

A minor product obtained from the chromatographic separation of complexes formed by the $Pt_2(DBA)_3$/DBBQ reaction was wine-red in color with a sharp absorption at 292 nm and a broad transition centered at 500 nm. The complex is EPR active, giving a spectrum that would be typical of a single DBSQ ligand chelated to a diamagnetic Pt center. The spectrum has a $g$-value of 1.9975 with coupling to one ring proton of 3.3 G and coupling to $^{195}$Pt ($I = {}^1/_2$) of 17.5 G. Infrared spectra obtained on the complex are similar to spectra of $Pt(DBSQ)_2$ and $Pd_2[Pd(DBSQ)_2]_2$, but little more is known about the product. A possibility considered was that it might be the one-electron reduction product $Pt(DBSQ)(DBCat)^-$; however, the electrochemistry on the complex was considerably different than that of $Pt(DBSQ)_2$. Cyclic voltammograms recorded on the compound show a reversible reduction at −0.500 V, an irreversible reduction at −1.150 V, and an irreversible oxidation at +0.830 V. A more likely form for the complex is $Pt[Pt(DBSQ)_2]_2$, with a structure that is similar to $Pd_2[Pd(DBSQ)_2]_2$ but with one of the bridging Pd atoms removed.

## Discussion

Studies on the quinone complexes of Ni, Pd, and Pt add to the information obtained on the dithiolene and diimine complexes of these metals. The quinone ligands have been considered as "noninnocent" and "dioxolene" in their coordination with transition metals, but there are very few cases where properties of the complex fail to point to a specific ligand charge. In many cases where charge distribution is ambiguous, supplementary spectroscopic indicators of metal or ligand charge (i.e. Mossbauer, EPR) are not available. Quinone complexes which have been

---

(19) Gozum, J. E.; Pollina, D. M.; Jensen, J. A.; Girolami, G. S. *J. Am. Chem. Soc.* **1988**, *110*, 2688.

shown to have extensively delocalized electronic structures occur most commonly for Ru and Os, metals which have valence orbital energies that are particularly close to the quinone $\pi$-orbital energy and for which orbital symmetry combinations are appropriate for metal–quinone delocalization.[20] Complexes of Ni, Pd, and Pt have now been prepared with 3,5-di-*tert*-butyl-1,2-benzoquinone and the zerovalent form of the metal to give bis(semiquinone) products. In the case of nickel, $Ni(DBSQ)_2$ was found to be tetrameric in structure, with octahedrally coordinated Ni(II) ions and weak antiferromagnetic exchange between the radical ligands and the paramagnetic metals.[4,21] This results from the strong tendency for Ni(II) to be octahedrally coordinated in complexes containing oxygen-donor ligands and the availability of the oxygen atom at Cl of the semiquinone for bridging interactions. In contrast, $Ni(3,6\text{-}DBSQ)_2$ is planar and monomeric due to steric protection at both oxygen sites by adjacent *tert*-butyl substituents.[22] The Pd and Pt complexes are different in structure from $[Ni(3,5\text{-}DBSQ)_2]_4$ but appear to be similar in charge distribution. This appears in the structural features of the semiquinone ligands, but it is most evident from the NMR spectrum of $Pd(DBSQ)_2$. Even though both complexes appear diamagnetic from Faraday balance measurements, NMR spectra on $Pd(DBSQ)_2$ indicate a residual low-level paramagnetism. Spin coupling between radical ligands is propagated through the "bridging" metal ion. The exchange interaction is sufficiently strong for the Pt complex to quench residual paramagnetism resulting in clearly resolved NMR spectra for both isomeric forms of the planar complex. The Pd analog is less stable than the Pt complex toward long retention times on the chromatographic column, and it was not possible to resolve cis and trans isomers in this case. Broadening in the NMR spectrum of the mixture of isomers obtained chromatographically indicates that the SQ–SQ exchange through Pd is weaker than the exchange interaction through Pt. In the interest of extending the use of NMR as a probe for low-level paramagnetism, we have looked at a second example, $Cr(DBSQ)_3$.[6a,23] This complex is reported to be diamagnetic due to strong radical–metal exchange, while analogs prepared with tetrachlorosemiquinone and phenanthrenesemiquinone were found to be weakly paramagnetic. The NMR spectrum of $Cr(DBSQ)_3$ consists of two broad resonances in the *tert*-butyl region at 1.34 and 2.07 ppm at 25 °C in $CD_2Cl_2$. As temperature is decreased to −80 °C, the 1.34 ppm resonance remains fixed in position while the 2.07 ppm resonance moves upfield to 1.58 ppm. This appears to be an additional case where low-level paramagnetism can be resolved using NMR.

## Conclusions

Magnetic exchange between radical semiquinone ligands results in the near diamagnetism of both $Pd(DBSQ)_2$ and $Pt(DBSQ)_2$. Differences in the magnetic properties of the two complexes indicate a metal-dependence in the magnitude of the exchange interaction. This is an interesting reversal on the more usual situation where paramagnetic metal ions show superexchange through a bridging ligand. As charge-localized semiquinone complexes of Pd(II) and Pt(II), the electronic structures of the complexes differ from related diimine and 1,2-dithiolene complexes of the Ni, Pd, and Pt series. Related complexes containing metals to the left on the periodic table show a tendency toward high oxidation state metal ions stabilized by the strong $\pi$-donation effect of the catecholate ligands. The preference for the divalent, rather than the tetravalent, form of the metal ions included in this investigation reflects the decrease in metal orbital energy across the transition series, illustrating the periodic dependence upon charge distribution for the quinone complexes of the transition metals.

**Acknowledgment.** This research was supported by the National Science Foundation through Grants CHE-88-09923 and CHE-90-23636; salts of palladium and platinum were provided by Johnson Matthey, Inc., through their Metal Loan Program.

**Supplementary Material Available:** Tables giving crystal data and details of the structure determination, anisotropic thermal parameters, hydrogen atom locations, and bond lengths and angles for $Pd(DBSQ)_2$, $Pd_2[Pd(DBSQ)_2]_2$, and $Pt(DBSQ)_2$ (27 pages). Ordering information is given on any current masthead page.

---

(20) (a) Haga, M.; Dodsworth, E. S.; Lever, A. B. P. *Inorg. Chem.* **1986**, *25*, 447. (b) Haga, M.; Isobe, K.; Boone, S. R.; Pierpont, C. G. *Inorg. Chem.* **1990**, *29*, 3795.

(21) Buchanan, R. M.; Fitzgerald, B. J.; Pierpont, C. G. *Inorg. Chem.* **1979**, *18*, 3439.

(22) Abakumov, G. A. Submitted for publication.

(23) Sofen, S. R.; Ware, D. C.; Cooper, S. R.; Raymond, K. N. *Inorg. Chem.* **1979**, *18*, 234.